

*Supporting Information*

Leakage-proof nacre-like boron nitride nanosheet/phase change microcapsule  
composites with enhanced thermal conduction and thermal energy storage for  
advanced thermal managements

Xiangkai Hu, Rong Lin, Zhihai Cao\*

*State Key Laboratory of Bio-based Fiber Materials, Engineering Research Center for Eco-Dyeing & Finishing of Textiles, Ministry of Education, and Zhejiang Provincial Engineering Research Center for Green and Low-carbon Dyeing & Finishing, Zhejiang Sci-Tech University, Hangzhou, 310018, China*

\*Corresponding author: zhcao@zstu.edu.cn (Z. H. Cao).

**Supplementary Figures**

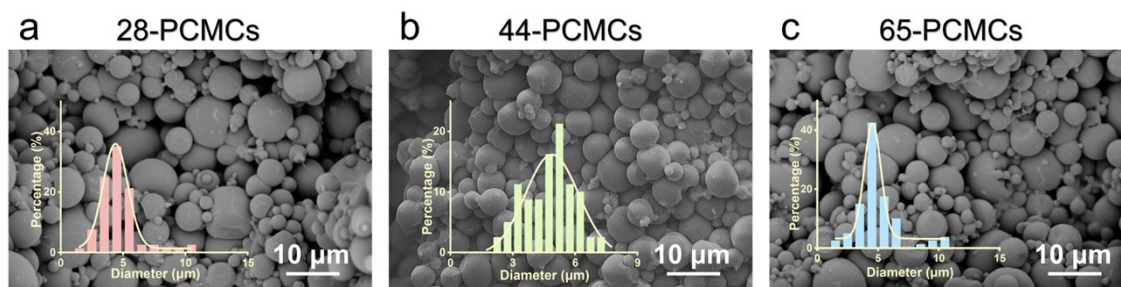


**Fig. S1** SEM images and number particle size distribution curves (insets) of T-PCMCs.

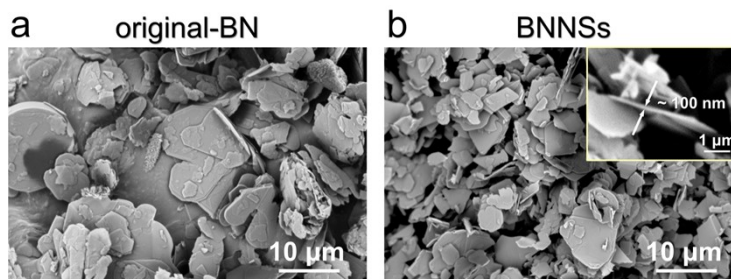


**Fig. S2** SEM images of (a) the original BN powder and (b) BNNSs (the inset in b is the magnified SEM image of BNNSs).

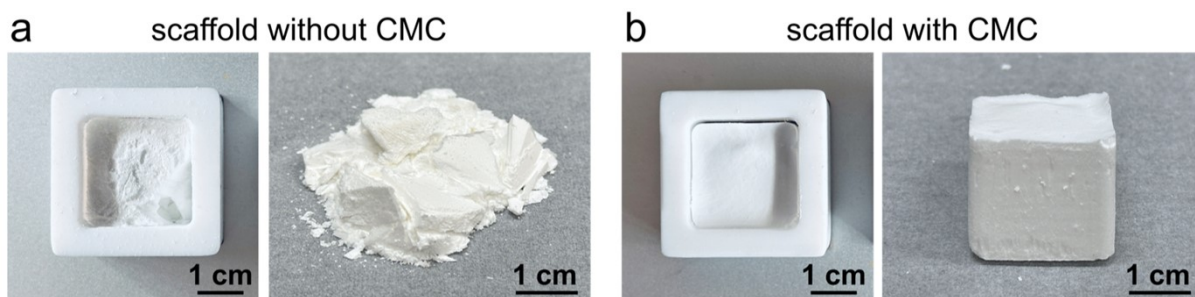


**Fig. S3** Photos of BNNS/PCMC scaffolds without CMC (a) and with CMC (b).

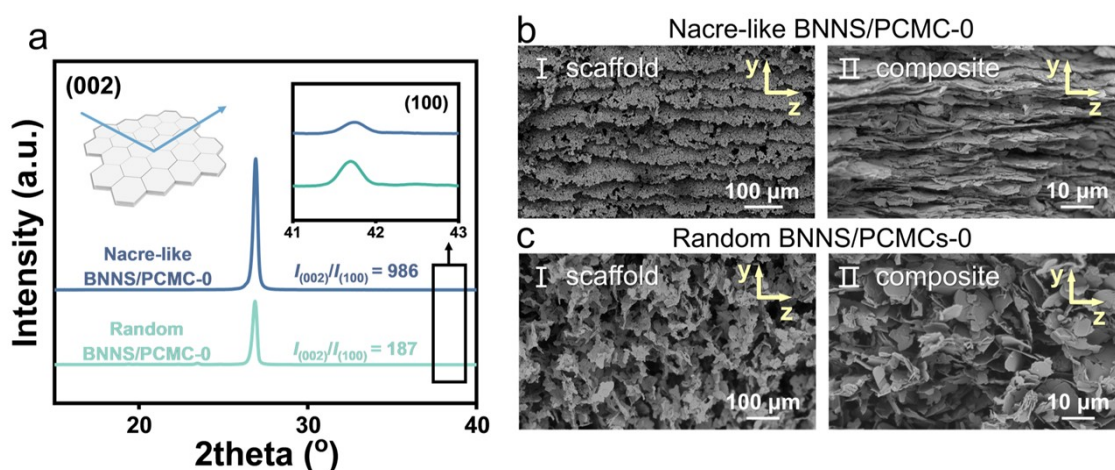


**Fig. S4** (a) XRD patterns of the nacre-like and random BNNS/PCMC-0 composites (the insets are the schematic representation of relationship between the (002) plane and XRD pattern (left) and the magnified XRD patterns of (100) plane (right), respectively). (b) SEM images of nacre-like BNNS/PCMC-0 scaffold (I) and composite (II). (c) SEM images of random BNNS/PCMC-0 scaffold (I) and composite (II).

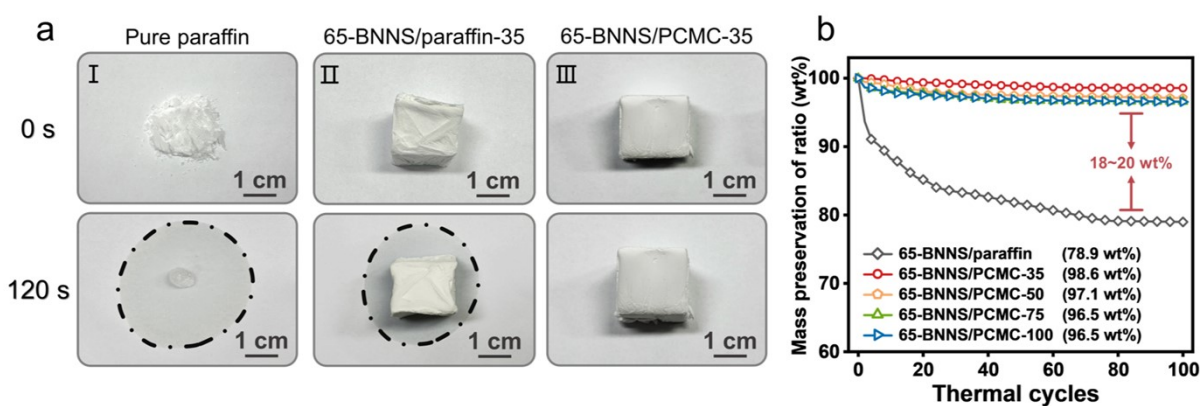


**Fig. S5** (a) Photos of the pure paraffin, 65-BNNS/paraffin-35 and nacre-like 65-BNNS/PCMC-35 composites before and after heated at 80 °C. (b) Mass preservation ratios of the nacre-like 65-

BNNS/PCMC-X and the 65-BNNS/paraffin-35 composites during 100 heating–cooling cycles.

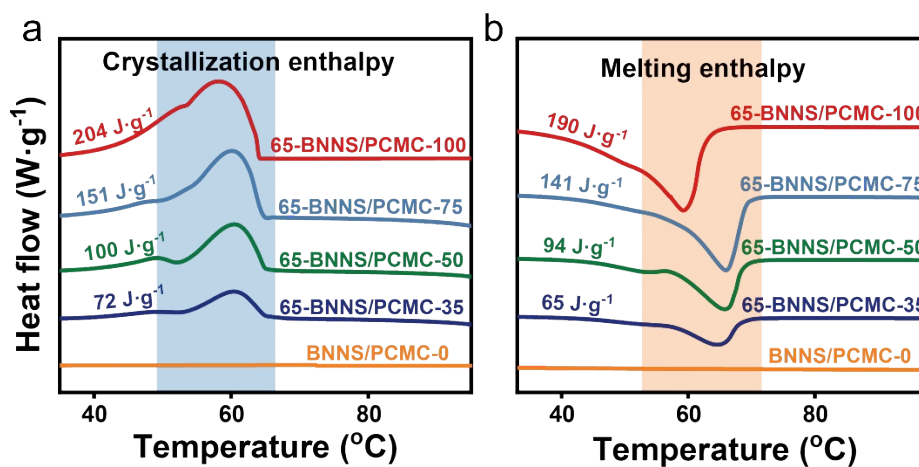


**Fig. S6** DSC thermograms of 65-BNNS/PCMC-X composites (a, crystallization process; b, melting process).

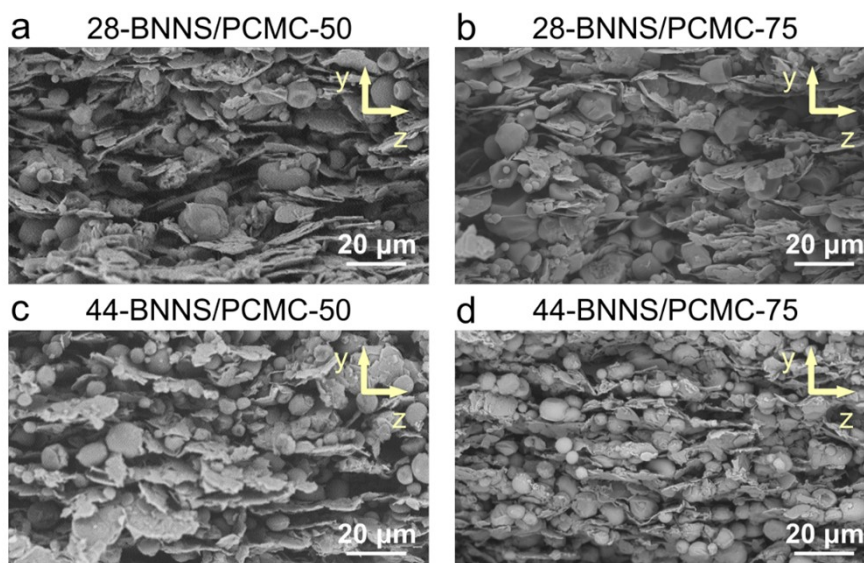


**Fig. S7** (a, b) SEM images of the y-z plane of nacre-like 28-BNNS/PCMC-X composites. (c, d) SEM images of the y-z plane of nacre-like 44-BNNS/PCMC-X composites.

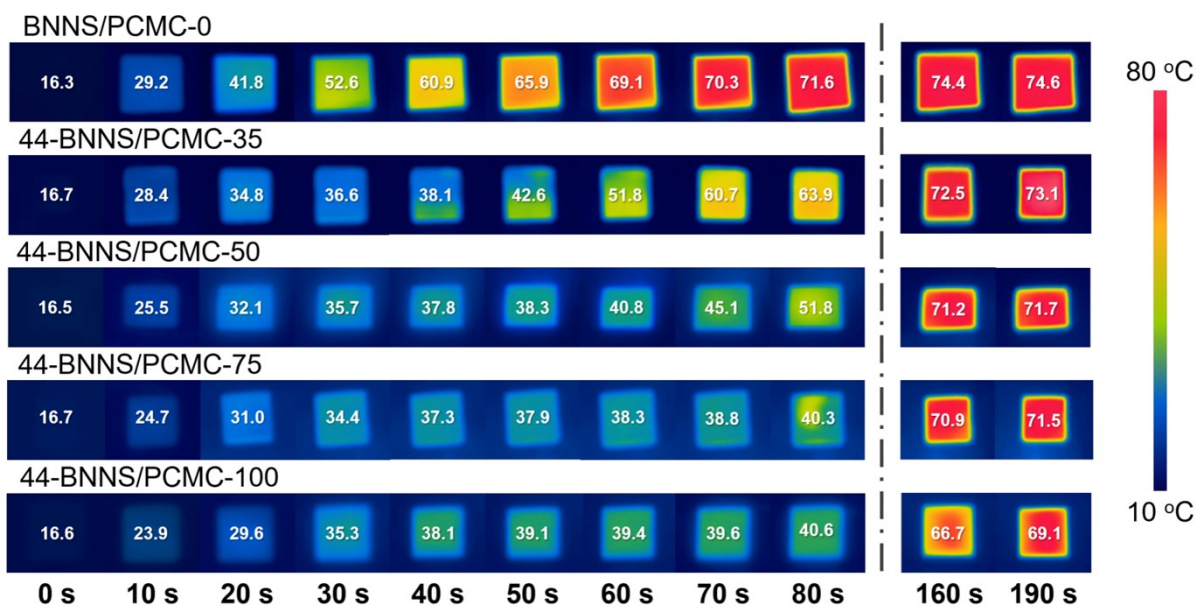


**Fig. S8** Time-dependent infrared images of the nacre-like 44-BNNS/PCMC-X composites heated on an 80 °C hot plate.

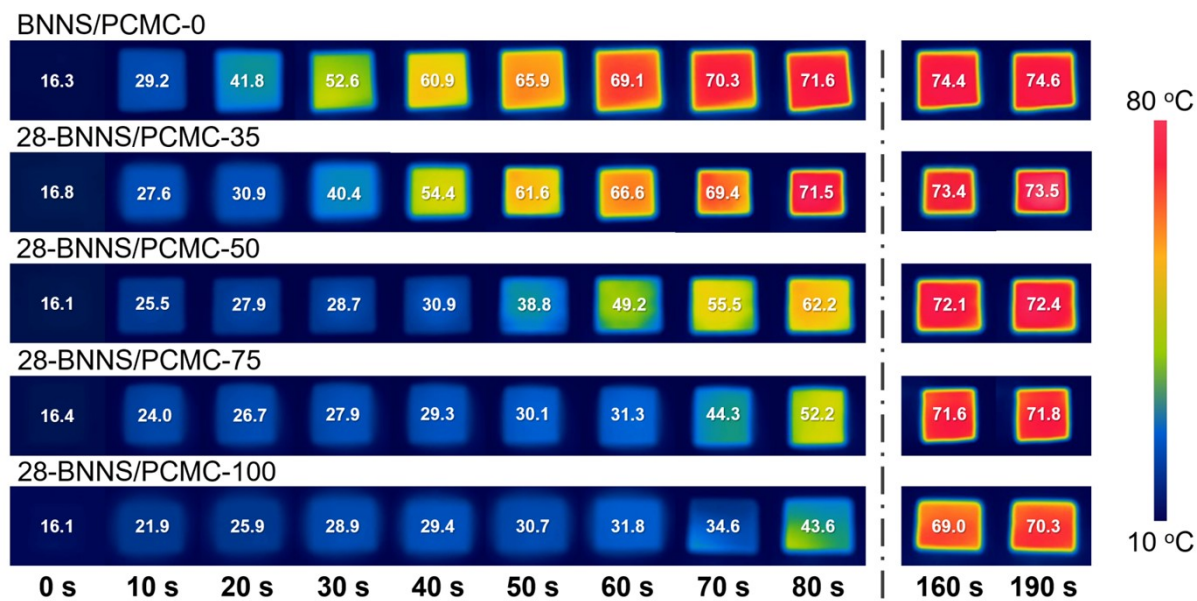


**Fig. S9** Time-dependent infrared images of the nacre-like 28-BNNS/PCMC-X composites heated on an 80 °C hot plate.

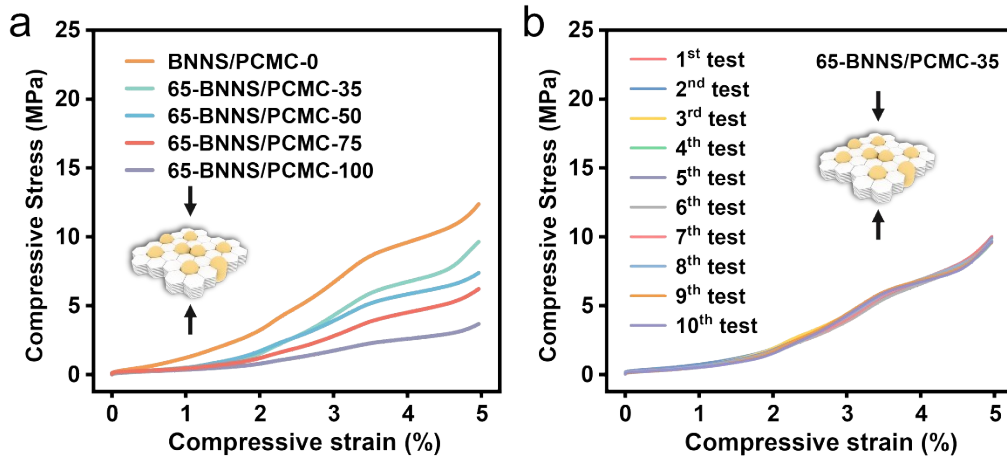


**Fig. S10** (a) Compressive performance of the nacre-like 65-BNNS/PCMC-X composites. (b) Repeated compressive performance of the 65-BNNS/PCMC-35 composite.

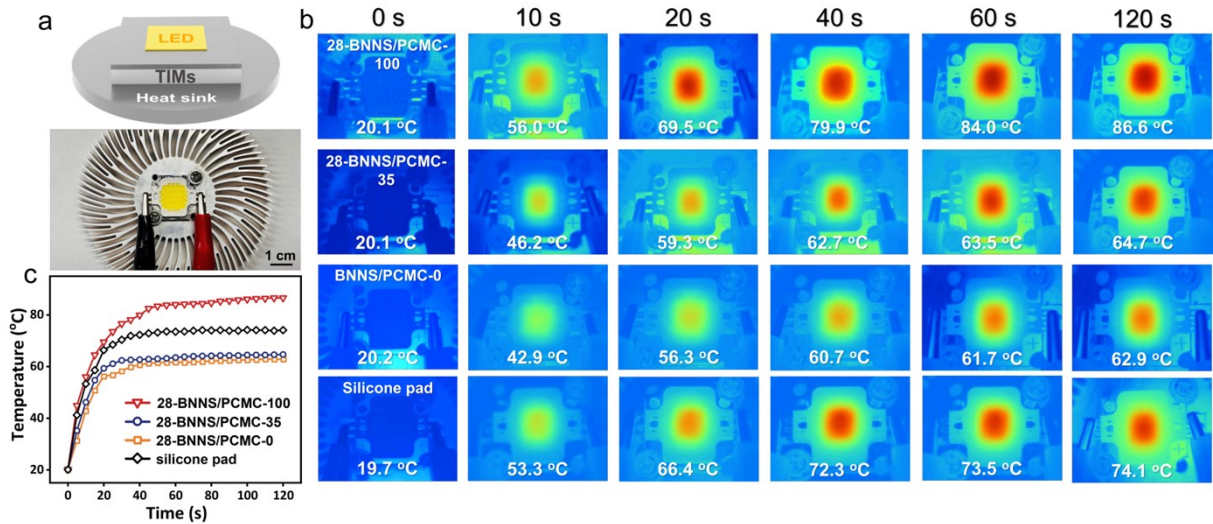


**Fig. S11** Application demonstration of the nacre-like 44-BNNS/PCMC composites as the TIMs: (a) The TIMs were integrated between the LED chip and heat sink for heat dissipation demonstration. (b) Time-dependent infrared images of the LED chips using the commercial silicone pad and nacre-like 44-BNNS/PCMC-X composites as the TIMs with a size of 20 mm  $\times$  20 mm  $\times$  2 mm.

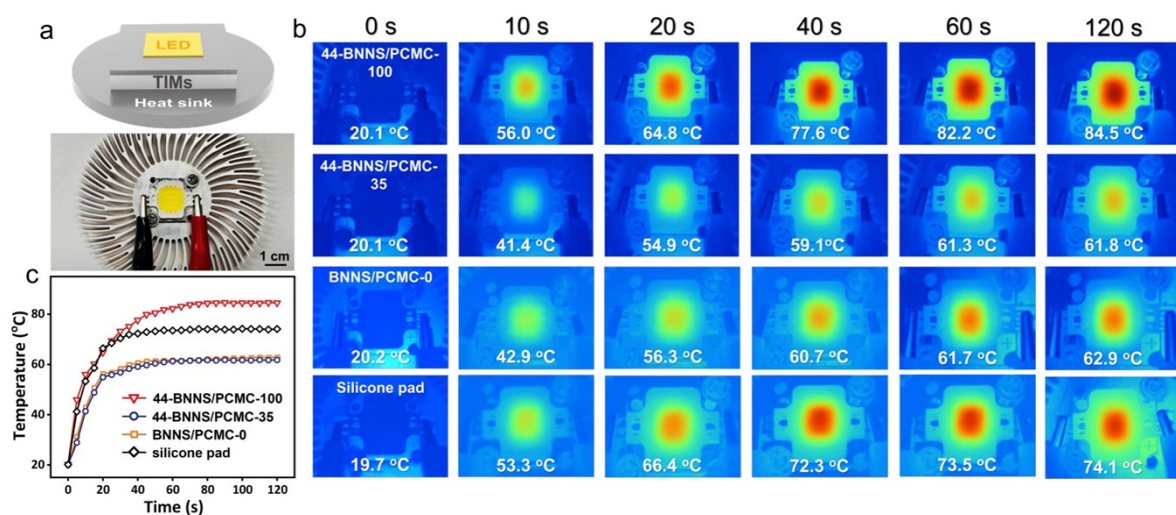


**Fig. S12** Application demonstration of the nacre-like 28-BNNS/PCMC composites as the TIMs: (a) The TIMs were integrated between the LED chip and heat sink for heat dissipation demonstration. (b) Time-dependent infrared images of the LED chips using the commercial silicone pad and nacre-like 28-BNNS/PCMC-X composites as the TIMs with a size of 20 mm  $\times$  20 mm  $\times$  2 mm.

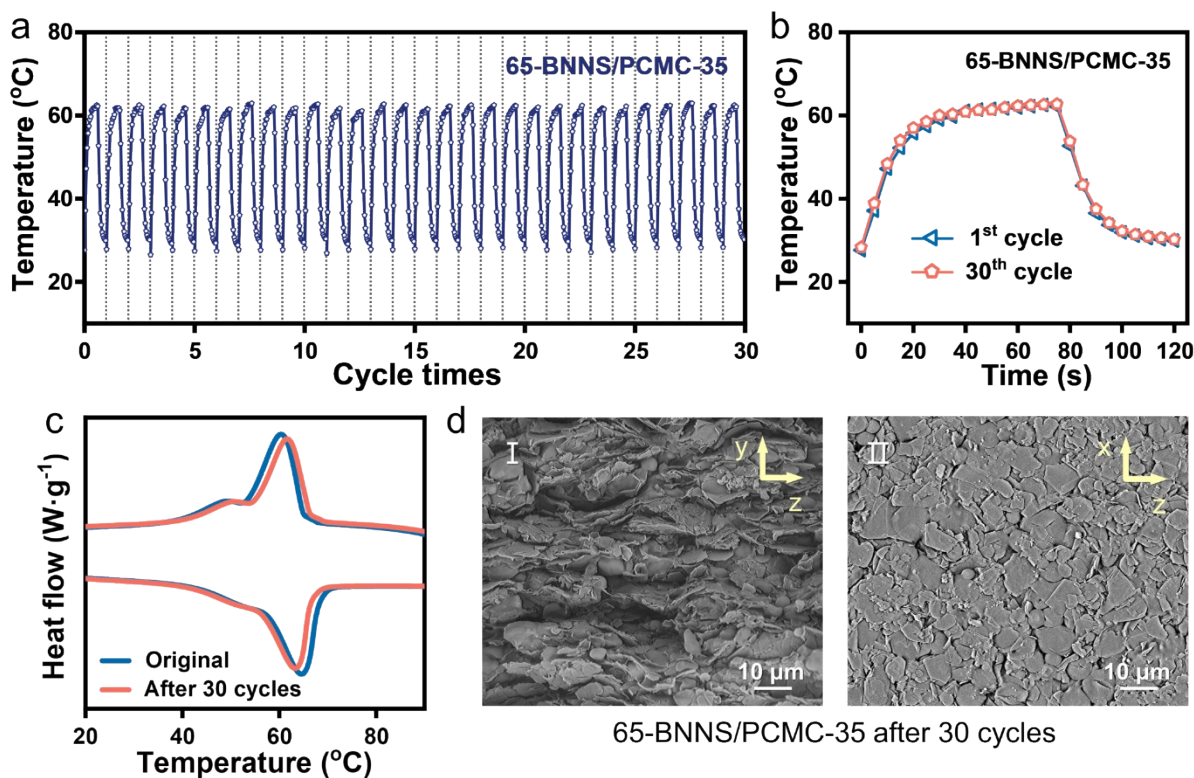


**Fig. S13** (a) Time-dependent surface temperature curves of the LED chip integrated with the nacre-like 65-BNNS/PCMC-35 composite during 30 on-off cycles. (b) The first and 30th time-dependent surface temperature curves of the LED chip integrated with the nacre-like 65-

BNNS/PCMC-35 composite. (c) DSC thermograms of the original and cycled 65-BNNS/PCMC-X composites. (d) SEM images of the cycled 65-BNNS/PCMC-35 composites (I, y-z plane; II, x-z plane).

## Supplementary Tables

**Table S1** Recipes for preparation of the BNNS/PCMC/CMC suspension

samples	BNNS (g)	CMC (g)	T-PCMCs (g)	H <sub>2</sub> O (g)
BNNS/PCMC-0	5.5	0.55	0	97.5
BNNS/PCMC-10	5.5	0.55	1.0 <sup>a</sup>	96.5
BNNS/PCMC-35	5.5	0.55	3.0	94.5
BNNS/PCMC-50	5.5	0.55	5.5	92.0
BNNS/PCMC-75	5.5	0.55	16.5	81.0

<sup>a</sup>65-PCMCs.

**Table S2** Properties of the 65-BNNS/PCMC-X composites

Samples	BNNS density (g·cm <sup>-3</sup> )	CMC density (g·cm <sup>-3</sup> )	65-PCMCs density (g·cm <sup>-3</sup> )	volume fraction of BN (vol%)
65-BNNS/PCMC-0				88
65-BNNS/PCMC-10				64
65-BNNS/PCMC-35	2.23	1.60	0.94	41
65-BNNS/PCMC-50				29
65-BNNS/PCMC-75				12

**Table S3** Thermal diffusivity values of the T-BNNS/PCMC-X composites

Nacre-like samples	$\alpha_{\text{In-plane}}$ (mm <sup>2</sup> ·s <sup>-1</sup> )	$\alpha_{\text{Through-plane}}$ (mm <sup>2</sup> ·s <sup>-1</sup> )
BNNS/PCMC-0	14.97 ± 0.28	0.99 ± 0.07
65-BNNS/PCMC-35	10.28 ± 0.31	1.36 ± 0.07
65-BNNS/PCMC-50	4.97 ± 0.24	1.28 ± 0.06
65-BNNS/PCMC-75	1.32 ± 0.17	0.22 ± 0.05
44-BNNS/PCMC-35	10.67 ± 0.23	1.19 ± 0.07
44-BNNS/PCMC-50	5.64 ± 0.18	1.19 ± 0.06
44-BNNS/PCMC-75	1.32 ± 0.15	0.30 ± 0.05
28-BNNS/PCMC-35	9.86 ± 0.23	1.29 ± 0.07
28-BNNS/PCMC-50	4.70 ± 0.18	1.27 ± 0.07

**Table S4** Comparison of TC values and latent heats of 65-BNNS/PCMC-X composites with those of the reported PCM/BN-based composites.

samples	BN content	PCM content	Isotropic TC ( $\text{W}\cdot\text{m}^{-1}\cdot\text{K}^{-1}$ )	latent heat ( $\text{J}\cdot\text{g}^{-1}$ )	References
PW-WPU-BN-2.5	25.2 wt%	71.5 wt%	0.96	149.0	40
PLR-PEG-40BN	9.1 wt%	68.2 wt%	1.70	104.2	41
PLR-PEG-60BN	13.0 wt%	65.2 wt%	2.72	91.2	41
PW-POE-BN	29.8 vol%	–	3.08	72.0	42
			through-plane:		
PEG-HBA	10 vol%	90 vol%	2.62;	121.9	43
			in-plane:		
			2.42		
PEG-CS-BN	1.9 wt%	93.7 wt%	0.4	165.3	44
PUPEG-PW@SiO <sub>2</sub> -BN	16.7 wt%	77.9 wt%	0.675	112.2	45
OCT-PVA-BN	25.4 wt%	72.7 wt%	0.839	172.0	46
PEG-MWCNTs-BN	10 wt%	–	1.15	109.1	47
65-BNNS/PCMC-35	41 vol%	53 vol%	7.89	72.0	
65-BNNS/PCMC-50	29 vol%	68 vol%	4.12	100.3	This work
65-BNNS/PCMC-75	12 vol%	86 vol%	1.14	151.1	

**Table S5** Parameters for fitting via the Foygel nonlinear model

Parameter	Nacre-like	Random
	65-BNNS/PCMC-X composites	65-BNNS/PCMC-X composites
$K_0$	13.85	9.81
$V_c$	0.012	0.012
$\tau$	1.015	1.095
$P$	50	50
$L$	5 $\mu\text{m}$	5 $\mu\text{m}$

$D$	$0.1 \mu\text{m}$	$0.1 \mu\text{m}$
$\bar{A}_s$	$2.8 \times 10^{-14} \text{m}^2$	$2.8 \times 10^{-14} \text{m}^2$

---